Hand-Wrist Bone Assesment for Automatic Age Identification

Riyanto Sigit [1)], Tri Harsono [2)], Farah Devi Isnanda [3)], Eva Dwi Rochmawati [4)], Elvi Triyana [5)], Cicik Nofindarwati [6)]
1,2,3,4,5,6) Dept. of Informatics and Computer Engineering Electronics Engineering Polytechnic Institute Of Surabaya, Indonesia
{[1]riyanto, [2]trison}@pens.ac.id, {[3]farancak, [4]evasip, [5]elvitryana, [6]ciciknofindarwati}@ce.student.pens.ac.id

Rosy Setiawati
Musculoskeletal Division, Radiology Departement Faculty of Medicine Airlangga University Of Surabaya, Indonesia
dr_setia76@yahoo.co.id

Abstract— Unknown people who have died in suspicious circumstances or in mass disaster often have no evidence to indicate chronological age. Using bone has been being mostly used by an experienced doctor to identify age since it provides the most accurate result compared to other diagnoses. However, due to manual identification, the doctor requires tremendous amount of time and the result is highly subjective to the doctor decisions and experience. In this paper, an automatic identification of person age is performed only from a hand-wrist bone structure. It provides a simpler way and reliable as compared to use full-hand bone structure. An active contour with balloons model is studied to extract hand-wrist bone parts namely epiphysis and metaphysis. From these parts, the width ratio is employed to identify person age. Experiments show encouraging results for the proposed method to automatically identify person age. We believe this can benefit for the future of forensic identification.

Keywords-*automatic age identification, hand-wrist bone, bone age assesment, balloons models, active contour*.

I. INTRODUCTION

Identification of a person age taken from hand-wrist bone is often carried out by an experienced doctor. Hand-wrist bone is selected as compared to other human parts such as tooth since it provides the most accurate result for the chronological age of an unknown subject in criminal investigation [1] [2]. Though the doctors need tremendous amount of time to identify person age, age identification from hand-wrist bone is still heavily used today, which is usually achieved by comparing a x-ray image of hand-wrist with the Greulich and Pyle's book to analyze the age [3].

Unknown people who have died in suspicious circumstances or in mass disaster [4] often lack evidence to indicate the birth date which can be presented in the criminal courts or for further investigation. The age estimation can be clearly expressed using hand-wrist bone and it could provide a reliable way since the hand-wrist bone fully structure often remain undamaged, as compared to other diagnoses such as tooth assesment.

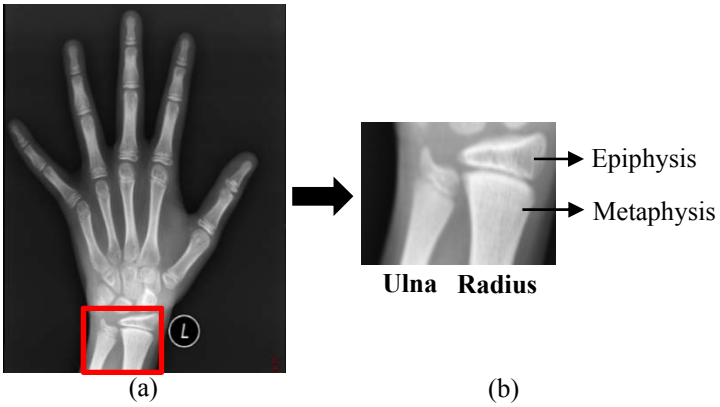

Fig.1. Identification of person age using only hand-wrist bone structure. (a) X-ray image and (b) hand-wrist part. Note that using only hand-wrist bone structure provide a simpler way as compared to fully hand bone structure.

Despite the fact that manual hand-wrist bone identification requires tremendous amount of time [5], it also prones to the observer's variability and could decrease the accuracy of bone assesment at the development stage. This means, it is largely limited to subjective decisions and depends on the experience of the radiologists or doctors who assess the bone. Therefore, an automatic person age assessment is ultimately important to be studied.

Previous work on automatic bone assessment has been studied by [6] and shows it can identify age relatively well by comparing directly from the specified references. Using fully hand bone structure is however difficult to achieve in practice as those bones prone to be damaged due to high collision with other materials, such as in disaster circumtances.

In this paper, automatic identification of person age is performed only from hand-wrist bone structure. Hand-wrist bone structure is shown in Fig. 1. This method has several advantages; First, it provides a simpler way as compared to using fully hand bone structure; Second, hand-wrist bone structure is relatively reliable as this bone often remain undamaged; Third, automatic person age identification is studied.

In order to automatically identify person age, initially an x-ray color image is converted into a grayscale. The hand-wrist

bone structure is then heuristically extracted from the grayscale image. Two balloons model active-contour are generated on the radius bone to extract epiphysis and metaphysis parts. An active contour is employed as it could perform fairly well on noisy image. However, the difficulty of growing contour on concave-shape object is well-known in active contour. This can therefore be solved using balloons model [7] to predict an accurate contour. The model work by minimizing the specified energy for the contour to expand. The final contour should have the highest energy for the iteration to stop [8] [9]. The width ratio of metaphysis and epiphysis parts are then used to identify the person age. Our method show relatively well to automatically identify person age using only hand-wrist bone structure.

II. RELATED WORK

The related work is Forensic Age Estimation (FAE) is not an introduction to a new field of skill in forensic science and judiciary history, as the eruption of the second molar was used in the Roman Empire as an indicator for calling young males for military service [10] In the nineteenth- century, age was estimated by dentists, and tooth eruption was considered to be a reliable method to detect the age of a child. In that era, the minimum criminal age was calculated to be 7 years old in Britain. However, some experts have objected to this method for the estimation of age. In 1846, Pedro Mata expressed his concern about estimating age based only on tooth eruption [11]. Angerer was the first person who stated that the carpus bone in the hand is an indicator for the estimation of age in young people [12].

Nurpadmi et al [13] applied segmentation of tibia bone image by using active contour models, and Zinah Rajab Hussein, et al [14] applied a preprocessing extraction contour for noisy ecocardiography image. The active contour model originally introduced by Kass has been further developed by modified in recent years. The balloon model or the expanding snake mode [15] is one of the examples of this. Unlike, the traditional snake that shrinks wraps to the image boundary, this snake model expands outwards. This model is based on an additional inflation force applied to give stable results. An active contour model which is not close to contours is not attracted by them. The curve behaves like a balloon which is inflated. When it passes by edges, will not be trapped by spurious edges and only is stopped when the edge is strong. The initial guess of the curve not necessarily is close to the desired solution. Pressure force is added to the internal and external forces.

Thus, the method used in the present study was determining the initial centers of the boundary. After that, the morphological operations were applied to eliminate the noise and to convert it into binary image. Finally, boundary and active contour models were used to detect and reconstruct the imprecise border. It is believed that this technique can detect the boundary of bone age image very precisely.

III. METHODOLOGY

Figure 2 shows the diagram of the aforementioned algorithm.There are various methods and algorithms to boundary the bone age image [1] [9]. In this algorithm, active contour models were used to automatically detect and reconstruct disconnecting as well as detect the center boundary of the bone age image.

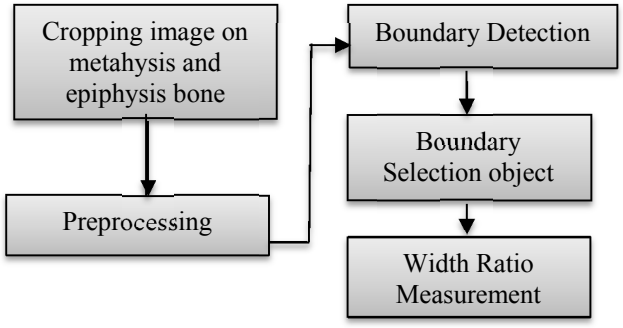

Fig.2. Schematic Diagram of the algorithm

A. Cropping Image

In this research, metaphysis and epiphysis bone were used on the right hand wrist bone to determine the age. So metaphysis and epiphysis bone were cropped on the right hand wrist bone by using the cropping image technique.

There are two types of crop techniques; the manual crop technique and the automatic ones. In this study experiment, the manual crop technique is used by cropping the image using the ROI (Region of Interest) rectangle shape. This process is used to separate merely on epiphysis and metaphysis bone with the other parts.

The algorithm of the image cropping:

1. Call mouse_callback function to select the bone on the bone age image.
2. Draw the box with cvRect function where this function as a pointer that contains the value of x and y of the box.
3. Resize the image with the region of interest (ROI) of the rectangle.
4. Display an image with key on a mouse event condition

Figure 3 shows the result from cropping image merely on the metaphysis and epiphysis bone.

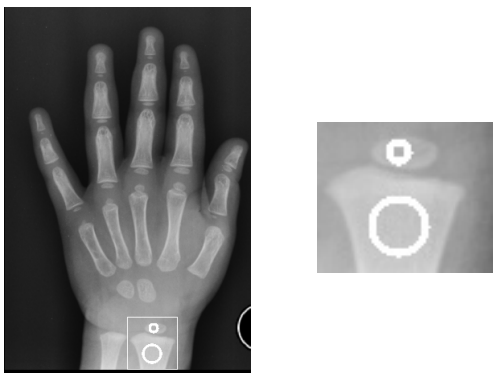

(a) (b)

Fig.3. (a) Original image on bone age image (b) Result from image cropping

B. Edge Detection and Morphological Filtering

The second step is pre-processing using morphological filter and edge detection of the object's image. Morphological filtering can be reduces the noise and clarify the border of the image. On morphology, an image expressed as a set of discrete coordinates. In this case, the set point or pixel-related objects on the image. Morphological operation using two inputs sets a binary image and the kernel (called structure-forming element). Whereas, edge detection method is using canny edge detection. Canny algorithm approach was done by convolution function image with a structuring element of morphology and their derivatives.

Eq. 1 below shows how to calculate or determine the values of each element in a opening operation:

$$X^B = (X \ominus B^S) \oplus B \qquad (1)$$

Where:

X^B = set of X

B^S = particles

In this research, using 3x3 kernel of a morphological filter that consists of 8 points is shows on Figure 5:

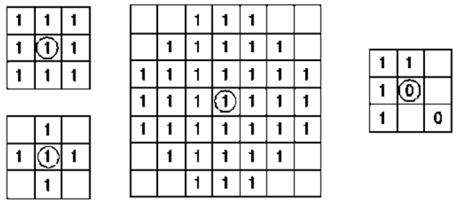

Fig.4. Example result from 3x3 kernel of morphological filter on the image pixel

Figure 4 depicts the formulation of morpgological filter image with image pixel value of Morphological kernel. It is shown in Figure 4 that the result of elements of structuring elements (SE) could be worth 1, 0 and don't care. The values don't care are usually marked with the value of the element is emptied. Excess data is a result of structuring elements can be reduced by reducing the outer portion of the same length so that the results can be seen in Figure 5 below:

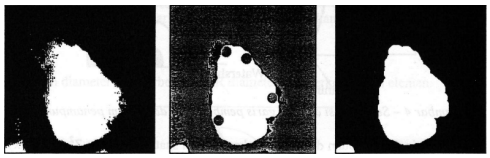

Fig.5. Reduction results pixels value of morphological filter.

Figure 6 below shows the result of dilation operation of hand-wrist image to reduce the noise.

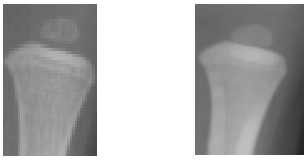

(a) (b)

Fig.6. (a) Original image, (b) Result from dilation operation.

The steps of canny edge detection are:

1. Remove noise contained in the image by implementing a Morphological filter. This process produces an image that looks a little blurry. It is intended to get the real image edges. If it is not done then the fine lines will also be detected as an edge.
2. Perform the edge detection by one of edge detection operators such as Roberts, Prewitt, or by doing a search Sobel horizontally (Gx) and vertically (Gy).
3. Determine the direction of edges found by the following formula on equation 2 below:

$$\theta = \arctan\left(\frac{Gy}{Gx}\right) \qquad (2)$$

Further split into 4 colors so that the lines with different directions and have different colors. The distribution is from 0 to 22.5 and 157.5 to 180 degrees yellow, green 22.5 to 67.5 and from 67.5 to 157.5 degrees red.

4. Far to the margins that arise by applying non-maximum suppression resulting in a slimmer line edges.

The implementation result of fourth step above is shown in Figure 7. The result from canny edge detection is converting RGB of image into binary image.

Fig.7. Result from canny edge detection of hand-wrist bones.

C. Boundary Detection

The third step is boundary object detection. First, the user is involved in determining point to start the process for detecting hand-wrist bone objects especially at the radius which metaphysis and epiphysis can be detected. From the points, process segmentation was started by using active contour models (snakes) to get a better segmentation of bone age.

Figure 8 shown the direction point which will start from an edge pixel and clockwise. Each pixel edge forms the boundary objects encoded with one of the eight chain code, and the chain code represents the object with the boundary first edge pixel coordinates, followed by a list of the next chain code [8].

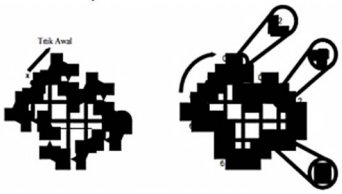

Fig.8. Encoding object with the boundary chain code

Figure 9 shown the object selection is done by initializing the starting point in the middle of the object and the edge border boundary of objects to produce the position accuracy edge boundary object of the segmentation process.

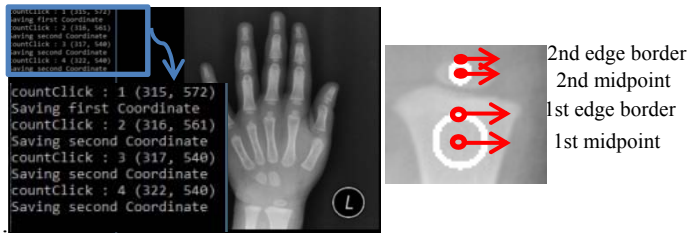

(a) (b)

Fig.9. Result from boundary object: (a) initialization edge midpoint and (b) the form of calculation results point

D. *Boundary Selection Object*

Boundary selection object is the fourth step. This method used active contour models (snakes). Figure 10 below shows a mathematical model of energy snakes, where Eint, Eimage and Econ represented the internal and external energy from active contour models.

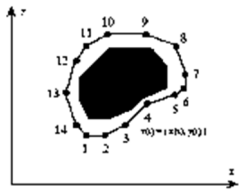

Fig.10. Snakes equation

Parameter active contour sets of coordinate points on contour controlled can be defined on eq. 3 below:

$$\vec{v}(s) = \left(\vec{x}(s), \vec{y}(s)\right) \quad (3)$$

Where x(s) and y(s) is the x and y coordinates on the contour and s is the normalized index of the control points. Energy function described active contour consists of two components is the internal energy and external energy. Internal energy makes compact curve (elastic force) and a very sharp turn limits (bending force). External energy tends to make the curve moves to the object boundary [11][12].

Internal energy as the sum of the elastic energy and energy resiliency can be expressed on eq. 4 below:

$$E_{int} = E_{elastic} + E_{bend} = \propto (s) \left|\frac{dv}{ds}\right|^2 + \beta(s) \left|\frac{d^2v}{ds^2}\right|^2 \quad (4)$$

Where α(s) is continuity function (stretching) and β(s) is functions of bending.

External energy limits the deformability of curve, the restrictions provided by the external energy can take various forms including the spring and repulse. In effect, external energy has never been used because every form of external energy has certain purpose.

Snakes energy has equation that sum internal energy and external energy which is shown on eq. 5 below:

$$E_{snake} = \int_0^1 E_{snake}(v(s)).ds$$
$$= \int_0^1 \{E_{int}(v(s)) + E_{image}(v(s)) + E_{con}(v(s))\}.ds \quad (5)$$

Where v(s) is coordinate values (x (s), y (s)), with the value s =0,1, E_{int} is internal energy, E_{image} is image force and E_{con} is external energy.

The results obtained from the gaussian operation of hand-wrist image to polish the object research. The boundary process can be done by alpha, beta and gamma parameter.

In the present study, the OpenCV Library, which is a library for computer vision, is used. Meanwhile, to get the boundary contour and to reconstruct it, this library should be modified. Contour in this library that can be stored inside a memory storage is a sequence. A sequence in OpenCV is actually a linked list [7].

In this research, movement energy using quadrant cartesian can be used to movement of baloon models. First step, calculation of points forming the circle in Figure 2.1 (b) uses the formula of circle which is shown on eq. 6:

$$\text{Distance} = \sqrt{(x_1 - x_0)^2 + (y_1 - y_0)^2} \quad (6)$$

The second step is calculation of the distance used as the radius of the circle to make a point of initials into a circle with a number of points as much as 360 circle axis 360 ° fit. Calculation of distance which shown on eq. 7 and 8:

$$x = center_x + distance(x1, y1, x0, y0) * \cos\left(\frac{360*\pi}{180}\right) \quad (7)$$

$$y = center_y + distance(x1, y1, x0, y0) * \sin\left(\frac{360*\pi}{180}\right) \quad (8)$$

When: x0 and y0 is first midpoint,x1 and y1 is second point

The third step is perform energy movement with gradient energy and quadrant cartesian rules. To run the energy gradient by gamma value can ellaborated the formula which shown on eq. 9 below:

$$E_{ext\_gradient} = -\gamma \sum_{i=0}^{n-1} (|G_x(x_i, y_i)|)^2 + |G_y(x_i, y_i)|^2)$$
$$<=> -\gamma \sum_{i=0}^{n-1} (|u_{x,i}\, G_x(P_i) + u_{y,i} G_y(P_i)|$$
$$\overrightarrow{u_i} = \frac{\overrightarrow{P(t_i)}}{|\overrightarrow{P(t_i)}|} \quad <=> -\gamma \sum_{i=0}^{n-1} \overrightarrow{u_i} \cdot \overrightarrow{G_y(P_i)} \quad (9)$$

The fourth step is finding the minimum energy of the boundary on the other border of the contour. In this method, *quadrant cartesian and active contour models* can be used to deformable curve the contour as shown in Figure 13.

Fig.11. Sample result using *quadrant cartesian and active contour models* to find minimum energy of boundary object in other border of the contour

E. *Wide-Ratio Features Measurement*

Part of the determination of age i.e. the ratio of the width of the metaphysical and epiphyseal based on the widest distance on x-axis. Calculation of the width of the search with the difference in the value of x with the following formulation:

1. Do the initialization point and midpoint edge on the metaphysical and the epiphysis bone image described at eq. 6

2. From the initials points of each image of the bones is referred to as the fingers to increase point form a circle. So the 2 initial starting point would be the appropriate point with an area of 360 full circle = 360° with a formula that has been spelled out in eq.7 and 8.
3. Provide a limit value of x1 and x2 is where the value of x1 as the value of the smallest width x or x < 0 and the value of x2 as the value of largest width or x > 0. So the calculation of the difference in width x is x2 – x1.
4. The width data of result is compared to reference data to determine the age.

The result of determine age which shown on figure 14 below:

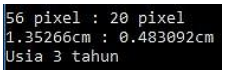

Fig.12. The results of the determination of the age

IV. EXPERIMENTAL RESULT

Before segmentation object of bone age only on metaphysis and epiphysis, there is one step that must be done is to determine the starting point iteration for the movement active contour models method. Table 1. shows the effect of initial iteration on the movement from active contour models method and result of object segmentation.

Table 1. Comparison between number of iterations and result object segmentation

Testing	Number of iterations	Result of segmentation	Ratio metaphysis : epiphysis (cm)	Time (second)
1.	1		0.57971 : 0.31401	25.7768
3.	10	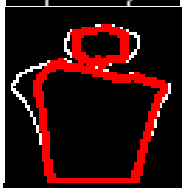	1.08696 : 0.434783	105.63
5.	25		1.28019 : 0.434783	209.387

From the table 1, it can be seen that if we use 25 number of iteration, we will get better segmentation on the metaphysis and epiphysis bone. In the 25 number of iteration produce width of the metaphysis and epiphysis which reaches nearly all edge of the bone that is 1.28019cm: 0.434783cm with the time is 209.387 seconds or nearly 4 minutes.

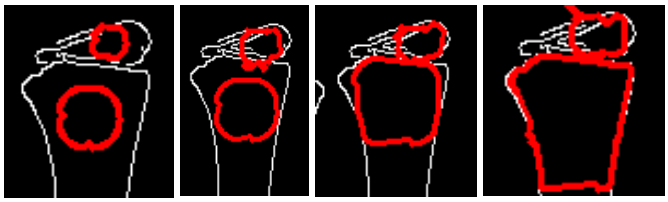

Fig.13. Movement by active contour models step by step

Result of the movement in the Fig.13 caused quadrant position of the x and y every points that has been initialized in the first active contour models process. When all of the points.

Testing identification of age based on the ratio width of the x coordinates. In the table 2. shows testing system with the 5 x-ray images of the patient's data.

Table 2. Testing system with bone age of patient's data

Age	X-ray File	Testing	Success (%)
3 years old	3th.bmp	5 data, 5 success	100 %
4 years old	4th.bmp	2 data, 1 success	50 %
6 years old	6th.bmp	5 data, 3 success	60 %
9 years old	9th.bmp	4 data, 2 success	50 %
13 years old	13th.bmp	3 data, 2 success	66,6%

From the table 2., it can be analyze that not all points will still on the edge of metaphysis and epiphysis bone. All of the points will move if there is not found edge in the bone's area. That is because of hand-wrist bone images not clearly. So, if we will get better segmentation every images must be set different threshold value and kernel of morphology. The average percentage of the system's success is 50% with 30x-ray images of the hand-wrist bone. This system is successfully identified 15 data that matched with age on x-ray image and 15 data errors. The smallest percentage error at the age is 3, 6 and 13 years old.

Table 3. Comparison average width of a metaphysis between system and reference

Age	Reference (cm)	System (cm)	Deviation (cm)	STD (5 testing)
3 years old	1,8	1,5942	0,20580	0,08191
4 years old	2,05	1,8116	0,23840	0,05124
6 years old	2,2	1,82125	0,3787	0,02160
9 years old	2,25	1,82609	0,42391	0,01323
13 years old	2,5	1,71498	0,78502	0,04184

Table 4. Comparison average width of a epiphysis between system and reference

Age	Reference (cm)	System (cm)	Deviation (cm)	STD (5 testing)
3 years old	1,2	0,700483	0,4995166	0,0241545
4 years old	1,55	1,19807	0,35193	0,5168203
6 years old	1,85	1,52657	0,32343	0,2552865
9 years old	2,15	1,487924	0,662076	0,169598
13 years old	2,7	1,599034	1,100966	0,133835

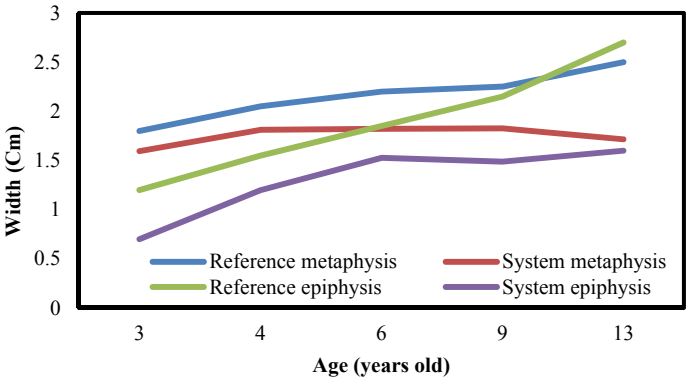

Fig.14. Chart of comparison metaphysis epiphysis between system and reference

From the fig.14. shows that in the 3 years until 10 years old have a small difference width reference and system that is 0.06 up to 0.4 on the metaphysis's width and the difference epiphysis's width is 0.02 up to 0.9. This is indicates that this method is effective to identification age from x-ray image of hand-wrist bone.

V. CONCLUSION

The proposed method presents solution for automatic identification of hand-wrist bone age. Morphology and edge detection methods can improve the picture quality. The proposed method can automatically detect mid points of the edge of the object, energy movement of balloons active contour model, calculate width and compare width of system with reference. Percentage success of the method used in the system to identify age by 50% of the total of 30 data is x-ray.

VI. ACKNOWLEDGMENT

The authors would like to thank the government of Indonesia (DIKTI) for the funding of this research through research grant.

REFERENCES

[1] Mardiati,Endah. *Hand-wrist Radiograph Analysis*. Bandung. Fakultas Kedokteran Gigi Universitas Padjajaran.

[2] Paewinsky, E., Pfeiffer, H., & Brinkmann, B. (2005). Quantification of secondary dentine formation from orthopantomograms—a contribution to forensic age estimation methods in adults. International journal of legal medicine, 119(1), 27-30.

[3] S.Idell Pyle, Alice W and William Walter Greulich. 1971. *A Radiographic Standard Of Reference The Growing Hand and Wrist.* The Press Of Case Western Reserve University, Cleveland.

[4] Warren M. W., K. R. Smith, P. R. Stubbefield, S. S. Martin, and H. A. Walsh-Haney, "Use of radiographic atlases in mass fatality," Journal of Forensic Sciences,vol. 45, no. 2, pp. 467–470, 2000.

[5] O'Keeffe, D. Denoising of carpal bones for computerised assessment of bone age [Ph.D.thesis], University of Canterbury Christchurch, Christchurch, New Zealand, 2010.

[6] Mansourvar, Marjan. 2014. *Bone Age Assesment Using Hand and Clavicle X-Ray Images*. The Faculty Of Computer Science And Information Technology University Of Malaya, Kuala Lumpur.

[7] A. Chopra, S. Rawat and P. Kumar, *Active Contours, Gvf and Balloon Model*, International Journal Of Computational Engineering Research,Mar-Apr 2012,Vol.2 Issue No.2 pp.403-407

[8] Yumiarty, Yuyun. 2010. Pembentukan Boundary Objek Pada Citra Digital Menggunakan Active Contour Models.

[9] Nurpadmi., Purnama,I Ketut Eddy. Segmentasi Citra Pada Citra CT Menggunakan Active Contour. Jurusan Teknik Elektro, FTI, ITS.

[10] Schmeling A, Reisinger W, Geserick G, Olze A (2008). Forensic Age estimation of liveadolescents and Young Adults. En: Forensic Pathology reviews. Vol 5.Editor:MichaelTsokos. Forensic Pathology Reviews, vol 5. Humana Press. 2008.

[11] Torroni, A., H.-J. Bandelt, et al. (2001). "A signal, from human mtDNA, of postglacial recolonization in Europe." The American Journal of Human Genetics 69(4): 844-852.

[12] Brothwell, D. R. (1981). Digging up bones: the excavation, treatment, and study of human skeletal remains. Cornell University Press.

[13] Indrawati. *Segmentasi Citra X-Ray Dari Citra CT Menggunakan Active Contour*. Program Studi Teknik Informatika Jurusan Teknik Elektro Politeknik Negeri Lhokseumawe.

[14] Zinah Rajab Hussein, Rahmita Wirza Rahmat, Lili Nurliyana, M. Iqbal Saripan and Mohd Zamrin Dimon, "Pre-processing Importance for Extracting Contours from Noisy Echocardiographic Images",IJCSNS International Journal of Computer Science and Network Security, VOL.9 No.3, March 2009, IJCSNS International Journal of Computer Science and Network Security, VOL.9 No.3, March 2009, March 5-20th 2009

[15] L. D. Cohen and I. Cohen, "Finite-element methods for active contour models and balloons for 2-D and 3-D images," IEEE Trans. Pattern Anal. Machine Intell., vol. 15, pp. 1131-1147, Nov. 1993.

[16] Lim, Resmana.,Santoso. *Verifikasi Personal Berdasarkan Citra Tangan Dengan Metode Filter Gabor*. Fakultas Teknik Elektro Universitas Kristen Petra.